Arabian Journal of Chemistry (2023) **16**, 105031

King Saud University

Arabian Journal of Chemistry

www.ksu.edu.sa
www.sciencedirect.com

ORIGINAL ARTICLE

Nanoparticles of (calcium/aluminum/CTAB) layered double hydroxide immobilization onto iron slag for removing of cadmium ions from aqueous environment

Teba S. Hussein *, **Ayad A.H. Faisal**

Department of Environmental Engineering, College of Engineering, University of Baghdad, Baghdad, Iraq

Received 23 December 2022; accepted 22 May 2023
Available online 29 May 2023

KEYWORDS

Alum;
Calcium;
Plaster kiln dust;
Layered double hydroxide;
CTAB surfactant;
Cadmium adsorption

Abstract The novel point of this study represents by manufacturing new material for treating of aqueous solution laden with cadmium ions. This can achieve through utilizing of alum as cheapest and available substance, plaster kiln dust wastes from gypsum industry, and cetyl trimethyl ammonium bromide surfactant in the preparation of nano-sized layered double hydroxide of aluminum and calcium in the existence of mentioned surfactant. The gel-solution of nanoparticles can be co-precipitated on the iron slag to obtain new sorbent identified "iron-slag coated with (calcium/aluminum- cetyl trimethyl ammonium bromide) layered double hydroxide" and composition of all materials was characterized by analysis of X-ray diffraction. The outcomes proved that the area of slag surfaces was increased significantly from 0.49 to 10.21 m^2/g due to the surfactant intercalation and precipitation of nanoparticles. The synthesis parameters require surfactant 0.035 g/50 mL, pH 10, molar ratio of (calcium/aluminum) 2, and mass of slag 1 g/50 mL. Batch tests proved that more than 99.3% cadmium can remove at time 60 min, initial pH 7, coated slag mass 0.5 g/50 mL, and speed 250 rpm for 50 mg/L initial concentration to obtain highest capacity of sorption of 14.50 mg/g. The measurements of kinetic tests were well followed the model of Pseudo second-order and; accordingly, the chemisorption mechanism will predominate the removal process. Model of intra-particle diffusion demonstrate that the electrostatic attraction, hydrogen bonding and diffusion are major mechanisms required in the cadmium removal onto the prepared sorbent. Also, Langmuir model is an ideal formula for representing the sorption data with determination coefficient = 0.99. Characterization tests certified that the nanoparticles on the slag can play a prime role in the enhancement of cadmium sorption. In addition, the exhausted sorbent can be regenerated

* Corresponding author.
E-mail address: teba.saadi.ts@gmail.com (T.S. Hussein).
Peer review under responsibility of King Saud University.

Production and hosting by Elsevier

https://doi.org/10.1016/j.arabjc.2023.105031

and its efficiency was not less than 83% for removal of cadmium after 9 regeneration cycles.

1. Introduction

Heavy metals like cadmium, nickel, zinc, copper, chromium and others, are closely related to the products of industrial society. These metals are utilized extensively in the antibacterial materials, electronic components, photosensitive materials, batteries, etc. If the wastewater laden with such toxic metals is dumped into the water resources and ecosystems, acute and chronic toxicity to health of public and ambient can be expected (Faisal and Nassir, 2016; Ghodsi et al., 2021; Shayesteh et al., 2021; Tang et al., 2020). Due to the toxicity of cadmium for living things, such metal has long been a cause for concern in the ecosystem. Malfunction of kidney, bronchitis, respiratory illnesses, and problems with reproduction can all be brought on by cadmium (Faisal et al., 2022a, 2022b, 2022c; Koldabadi et al., 2012). The permissible level for cadmium concentration in the surface water according to the environmental regulations must not be exceeding 0.005 mg/L (Faisal and Hmood, 2015). Thus, the metal removal especially cadmium ions from resources of water represents the unique task for recent researchers (Basibuyuk and Kalat, 2004).

There are numerous techniques for remediating of effluents laden with metals; however, the best one relies upon the contaminant content and the processing cost. Electroplating, chemical precipitation and ion exchange are familiar techniques that mostly applied to remove the hazardous metals. The technique of adsorption considers one of promising methods due to its resistance to poisonous substances, simplicity of design, and operation, as well as its low cost (Faisal et al., 2022a, 2022b, 2022c; Hilal et al., 2012). The prime sorbent applied historically in the remediation of metal ions – aqueous solution is the "Activated carbon" which cost varied from 1500 to 2000$ for each ton including 10–15% loss for covering the regeneration process (Samra et al., 2014). Utilization of cheapest sorbents like olive pips (Faisal et al., 2020) and date stones (Faisal et al., 2022a, 2022b, 2022c), or preparation efficient reactive materials from byproducts like cement kiln dust (Shihab and Faisal, 2022), sewage sludge (Faisal et al., 2022a, 2022b, 2022c) and waste foundry sand (Faisal and Ahmed, 2014) instead of high cost ones has been extensively studied. Also, nano-sized sorbents were applied in several researches like (Behbahani et al., 2022; Ghorbani-Kalhor et al., 2015; Zarezade et al., 2017) to treat wastewater laden with toxic metals.

Among the popular sorbents, layered double hydroxide (LDH) materials have extensively applied due to their high efficiency, easy in synthesis, and low cost (He et al., 2017; Zhao et al., 2011). LDHs are a wide class of ionic lamellar compounds consisted of layers charged positively with containing charge compensating anions and solvation molecules within the interlayer region, its similar to brucite structure in which trivalent metal ions partially substitute divalent cations. The general formula of LDHs may be described as $(M^{2+}_{1-x} M^{3+}_{x} (OH)_2)^{X+} (A^{m-})_{x/n}\cdot nH_2O]$, where M^{2+} and M^{3+} are metal cations which occupy octahedral holes in a brucite-like layer. These cations come from the divalent and trivalent metal salt utilized for preparing of LDHs (Zubair et al., 2017). The A^{m-} forms different types of organic or inorganic anion that situated in the hydrated interlayer. The replacement of M^{2+} by M^{3+} in the hydroxide layer brings about a positive charge, which can neutralize by (A^{m-}). The space of interlayer also includes molecules of water, hydrogen bonded to OH^- layer and/or to the anions interlayer (Normah et al., 2021). Several previous investigations (Faisal et al., 2022a, 2022b, 2022c; He et al., 2018; Liang et al., 2013; Tran et al., 2018; Zhao et al., 2011) are directed to prepare LDH from different materials and used to capture a wide board of chemicals. The introduction of cetyl trimethyl ammonium bromide (CTAB) bio-surfactant to the LDH composition can increase the sorption performance of prepared material especially this surfactant can classify as environmental friendly in its behavior (Kheradmand et al., 2023; Shayesteh et al., 2021, 2016).

Huge quantities of industrial by-products can be generated as solid wastes that accompanied the production of useful materials required for supporting the living development adopted by human. In this direction, iron slag is regarded as a solid waste byproduct resulted from manufacturing operations that occur in the iron and steel factories. According to earlier researches, almost 50 million tons of this slag are produced globally year. These substantial amounts can build up across huge tracts of land, rendering them unsuitable for agricultural use (Proctor et al., 2000; Tsakiridis et al., 2008). In addition, gypsum is the calcium sulfate dihydrate that must be calcined to produce stucco (i.e. calcium sulfates half hydrate). The calcination of one ton from gypsum leads to 0.85 ton of stucco and the remaining represents the particulate matters (known as plaster kiln dust, PKD) emitted as byproduct from gypsum plants. Millions tons of gypsum are produced in each year worldwide and; accordingly, one can forcast the dust quntity released into the ecosystem (Zwayen and Alhussainy, 2020).

This work concentrates on the preparation of novel sorbent from iron slag and plaster kiln dust to decrease the negative impacts of such solid wastes on the ecosystem and this represents a real application of sustainable concepts. The research idea requires to extract the calcium ions from PKD which mixed with aluminum ions from alum in the presence of certain surfactant to produce (Ca/Al-CTAB) LDH nanosized particles. These particles must be immobilized on the slag surfaces to prepare "iron-slag coated with (Ca/Al-CTAB)-LDH". Hence, the specific aims are included: i) development an innovative sorbent from combination of LDH and slag for treating of water contaminated with cadmium ions; ii) investigation the physiochemical characteristics of synthesized sorbent by "X-ray diffraction patterns (XRD)", "Brunauer–Emmett–Teller analysis (BET)", "field-emission scanning electron microscopy (FESEM)", "energy dispersive X-ray spectroscopy (FEEDX)", and "Fourier transform infrared spectra (FTIR)" to find the predominant mechanisms for removal process; iii) identification of suitable operation conditions for wastewater-coated slag interaction.

2. Experimental work

2.1. Materials

The PKD utilized in this work was collected from a plaster factory in the Kerbala Governorate-Iraq. To synthesize nanoparticles of (Ca/Al-CTAB)-LDH, calcium ions were extracted from PKD and added to the aluminum ions prepared by dissolving alum in distilled water (DW). The PKD is heterogeneous matter because it includes particles of various sizes; therefore, sieving is necessary to select particle between 0.6 and 1 mm (Colangelo and Cioffi, 2013). The $Al_2(SO_4)_3\cdot 14H_2O$ is chemical form for "Alum" used to prepare the solution rich with Al ions. The organic cationic surfactant named CTAB is obtained from Sigma Aldrich Chemise-Germany in the form of powder. The intercalation of CTAB can play a remarkable role in the expansion of interlayers for LDH, causing an obvious increase in the area of surface for coated slag.

Iron and steel factory in Babylon governorate, Iraq was the source for collecting the slag byproduct. To get rid of the fine powder, slag must be cleaned with DW; then, it must dry at

105 °C for 24 h. The characteristics of slag have specified at the Material Research Laboratories - Ministry of Science and Technology; Petroleum Development and Research Centre-Ministry of Oil; and Iraqi Geological Survey. The particles utilized in this study have sizes ranging from 0.6 to 1 mm; therefore, a geometric size of 0.775 mm. For iron, the bulk density, hydraulic conductivity, porosity, pH, ash content, and BET surface area have values of 2.026 g/cm^3, 2.69 $\times$ 10^{-3} m/s, 0.41, 8, 10% and 0.2571 m^2/g respectively.

In this investigation, cadmium (Cd) were selected to represent heavy metal. Stock solution (1000 mg/L) was prepared and must keep at room temperature to use it in the batch tests. The acidity of prepared solution can change by adding 1 M NaOH or HCl as needed to prevent cadmium ions from precipitating.

2.2. Choice of the material

The main goal for present research is the extraction of calcium from PKD byproduct rather than releasing it into the environment. In order to produce nanoparticles of LDH that are planted on the surfaces of the slag by co-precipitation and given the name "iron-slag coated with (Ca/Al-CTAB)-LDH", the CTAB surfactant is mixed with calcium and aluminum ions. This composite sorbent's capacity in the Cd^{+2} ions capturing from aqueous environment is primary guide for determining the optimal CTAB, Ca/Al ratio, solution pH, and iron slag dosage for its production. The following points and block diagram in Fig. 1 provide an explanation of the preparation approach:

1. One gram of PKD was mixed with one hundred milliliters of DW that contained 1.5 mL of 10% (v/v) HCl. Filtration with filter papers can separate the solid (filter cake) from this solution, which is rich in Ca^{+2} ions, after three hours of agitation at 250 rpm at room temperature.
2. To make an aluminum solution with varying molar concentrations, specific weight of alum must be dissolved in distilled water.
3. For the final solution to have different molar ratios of Ca/Al like 1, 2, and 3, the calcium solution that was obtained in step 1 must be mixed with the aluminum solution that was prepared in step 2.
4. 50 mL of the solution that had been prepared in step 3 contained two doses of CTAB, specifically 0.035 and 0.05 g. After that, either 0.5, 1 or 1.5 g of iron slag-based immobilized solid matrix were added to this solution.
5. In order to produce iron slag coated with nanoparticles of Ca + Al + CTAB, flasks must agitate at 250 rpm for three hours, and the solution was ultra-sonicated for 10 min to ensure the smoothing and dispersal of the nanoparticles. Hydroxide of sodium (1 M) can be used to raise the pH of the solution in step (4) to a variety of values, including 9, 10, and 11.

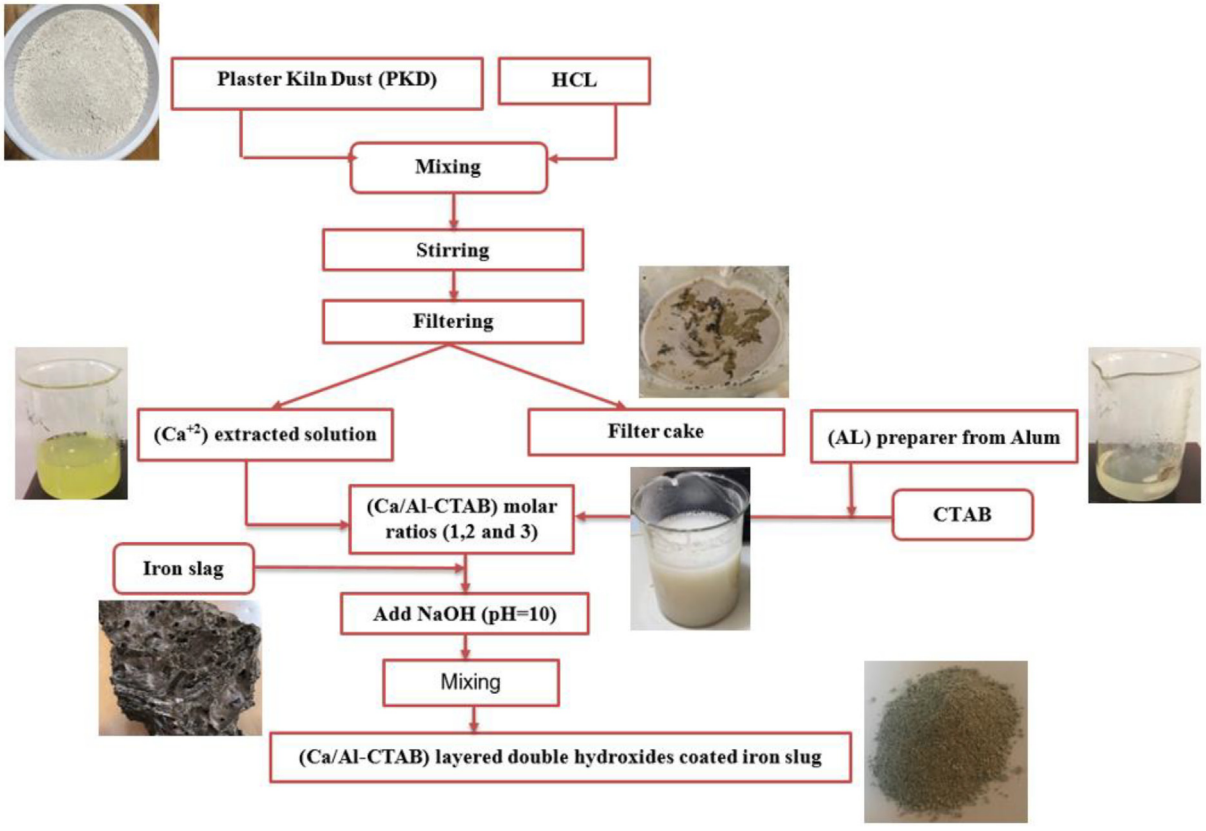

Fig. 1 Flowchart for manufacturing approach to prepare iron-slag coated with (Ca/Al-CTAB) LDH Nano particles.

6. Centrifugation was used to separate the coated iron slag from the solution. In order to use this slag in the subsequent batch sorption tests, it must be air dried for 24 h at 60 °C; consequently, the capability of coated slag to clean up cadmium-contaminated water should be specified.
7. The following analyses revealed the characteristics of the materials used to prepare coated slag:

a) FESEM was achieved by "SEM, Quanta200 [FEI, USA], NovaNanosem230 [FEI, USA] analysis under 10 KV voltage and a 6-mA flux".
b) FT-IR analysis was done using "Bruker Tensor 27 spectrophotometer with KBr pellet technique".
c) The BET analysis determines the area of specific surfaces using a surface area analyzer based on "nitrogen adsorption at 77 K, using an automatic Micrometrics 670-IR; 620-IR Imaging Model [Agilent, USA], Nano ZS [Malvern, UK]".
d) XRD analysis is used to find the components of used materials "D/MAX 2500 V/PC [Rigaku, Japan], D8 device".

2.3. Batch tests

Batch tests determine the equilibrium-kinetic data for the contact of cadmium ions with manufactured sorbents. To determine the optimal conditions for operation, like agitation time, initial pH, sorbent dosage, and speed of agitation, for a particular initial concentration (C_o) that is required to maximize removal efficiency for the target metal through sorption measurements. Flasks of 250 mL are supplied for batch tests, 50 mL volume (V) of polluted water with C_o 50 mg/L must be added to each flask, various dosages of coated slag were inserted, and the flasks must agitate for three hours at 250 rpm. After that, the solutions of flasks have filtered to isolate solids from water.

An "Atomic absorption spectrophotometer, AAS" can measure the metal residual concentration (C_e) in filtered solution. The sorbent's sorbed quantity can be calculated using the mass balance principle. The sorption study was applied at pH levels changing from 3 to 7, C_o varying from 50 to 300 mg/L, and sorbent dosage (m) ranging from 0.01 to 1 g/50 mL, with a contact time of 3 h. Each point in the sorption plots for batch tests under the influences of different operational conditions represents the average of 3 readings and statistical analysis signified that the percentage of error for these readings at any point is very low (less than one percent). Contaminant capturing onto the slag (q_e) can calculate for optimal conditions as follows (Wang and Wang, 2008):

$$q_e = (C_o - C_e)\frac{V}{m} \tag{1}$$

Model for sorption data is graphed among q_e and C_e; however, the following equation can be used to calculate the removal efficiency (R):

$$R = \frac{(C_o - C_e)}{C_o} \times 100 \tag{2}$$

3. Formulation of sorption outcomes

3.1. Adsorption isotherms

The mathematical basis for adsorption is an isotherm models that express the distribution of contaminant concentrations between solid particles and liquid phase at status of equilibrium for a specific temperature (Zheng et al., 2009). Two equilibrium relationships are applied as explained underneath (Nava-Andrade et al., 2021):

1) **Freundlich's model:** is the first non-linear expression for the sorption modeling, and its formula is as follows:

$$q_e = K_f C_e^{1/n} \tag{3}$$

where K_f is indictor to adsorption capacity and n is sorption intensity.

2) **Langmuir model:** is also non-linear expression for the sorption modeling that bears Irving Langmuir's name and published in 1916 with following formula:

$$q_e = \frac{q_m b C_e}{1 + bC_e} \tag{4}$$

where q_m is highest capacity of sorption and b is affinity between contaminant and sorbent. It specifically explains sorption data for uniform adsorption energies on sorbent surfaces. Additionally, this model can account for the case where chemical species that have been adsorbed on nearby sites do not interact.

3.2. Adsorption kinetics

It is necessary to specify residence duration in the sorption system, design suitable sorption process, and comprehend the controlling sorption mechanisms; thus, kinetic study is required to determine the contaminant's uptake rate (Qiu et al., 2009). Two kinetic expressions have been applied to the current sorption measurements:

1) **Pseudo first order kinetic model:** It describes in Eq. (5) (Dinari and Neamati, 2020):

$$q_t = q_e(1 - e^{-k_1 t}) \tag{5}$$

where q_t is the adsorbed contaminant at time t (mg/g), q_e is adsorbed contaminant at equilibrium (mg/g), and k_1 is the rate constant of this model (min^{-1}).

2) **Pseudo second order kinetic model:** It works for a monolayer of chemical onto sorbent grain without reaction between chemical species. This model's non-linear form is as follows:

$$q_t = \frac{t}{\left(\frac{1}{k_2 q_e^2} + \frac{t}{q_e}\right)} \quad (6)$$

where k_2 is the rate constant (g.mg^{-1} min^{-1}).

4. Results and discussion

4.1. Characterization analyses

The results of the FT-IR analysis for wavenumbers ranging from 400 to 4000 cm^{-1} (Fig. 2) was used to identify the working functional groups for PKD, coated iron slag, coated iron slag loaded with Cd^{+2} ions, and virgin iron slag. According to the spectra, the OH group is represented by a broad and strong peak at wavenumber 3442.3 cm^{-1} (Faisal and Naji, 2019). The C—C group vibration can be linked to peak values of 554.4, 675.93, 704.9, 811.8, and 894.7 cm^{-1} that were found. C—O group vibration can be used to identify the peak values of 1149.4, 1260.25, 1265.07, 1290.14, and 1308.5 cm^{-1} that were identified (Le-ping et al., 2010). At 1560.13 cm^{-1}, an olefinic C═C stretching band can be seen, and its conjugation with a C═O or C═C bond can cause a clear shift to lower wavenumbers. As a result, the principal functional groups found in the current materials are O—H, C═C, C═O, C—C, and C—O. Appearance of peaks at 2345.16 and 2358.5 cm^{-1} demonstrated to the existing of C-N vibration in tertiary amines. This means that the grains of coated slag are maintained on their structure through the interaction with solution contained the target metal (Khitous et al., 2016). Some peaks have observable shifts in the wavenumbers, referring that there is strong affinity by target metal and available functional groups (Shah et al., 2021). In addition, the bands intensities for complexes of metal-hydroxide can be significantly varied. This proposes that the ion exchange may be the prime process enhanced the elimination of cadmium from the water. According to the FT-IR spectrum of a reactive material's chemistry, hydrogen bonding and electrostatic interaction can also support this elimination (Khitous et al., 2016).

The results of "X-ray diffraction (XRD) analysis" is very essential for specifying and identifying the mineralogical composition of materials used in the preparation of present sorbent. In Fig. 3a, the PKD, virgin iron-slag, and Fig. 3b, a coated iron-slag XRD patterns were displayed. In order to create a plot relating the intensity of the diffracted beam to (2θ), the material sample in this test is subjected to a collimated beam of parallel X-rays and diffracted beams of varying intensities. With Cu K radiation and an X-ray diffractometer (40 mA, 40 kV), the records with 2θ ranged from 5° to 80°. Based on International Centre for Diffraction Data, ICDD databases, the XRD pattern of PKD had peaks that correspond to many compounds like gypsum, montmorillonite, calcium sulfate, iron oxide, and quartz. Also, Fig. 3a certifies the presence of many metal oxides in the composition of iron slag like manganese, aluminum, calcium, iron, and silica. Depended on the "Joint Committee on Powder Diffraction Standards, JCPDSs", the XRD analysis for coated slag proved the appearance of several reflections at intensities of 11.31, 22.69, 25.50, 31.74, 38.87, 40.98, 45.47, 52.54, and 57.32 which identical to the nanoparticles of Ca + Al + CTAB precipitated on the slag surfaces. These reflections represent new sites formed on surface of iron-slag as a result of the conversion of inert iron-slag to reactive material. As a result, new sites will be in charge of removing Cd contaminants from aqueous solutions. Because of the development of diffraction peaks hydrotalcite-like compounds could occur (Guo et al., 2012), and this proves the success of nanoparticles plantation (Ca/Al-CTAB) LDH.

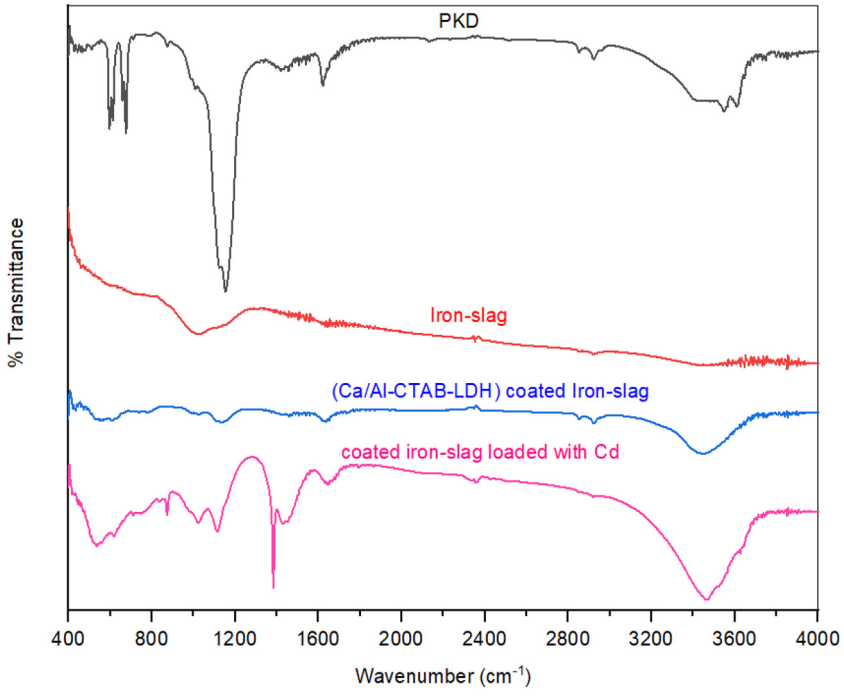

Fig. 2 FT-IR spectra for plaster dust, iron-slag, coated slag, and coated slag loaded with cadmium ions.

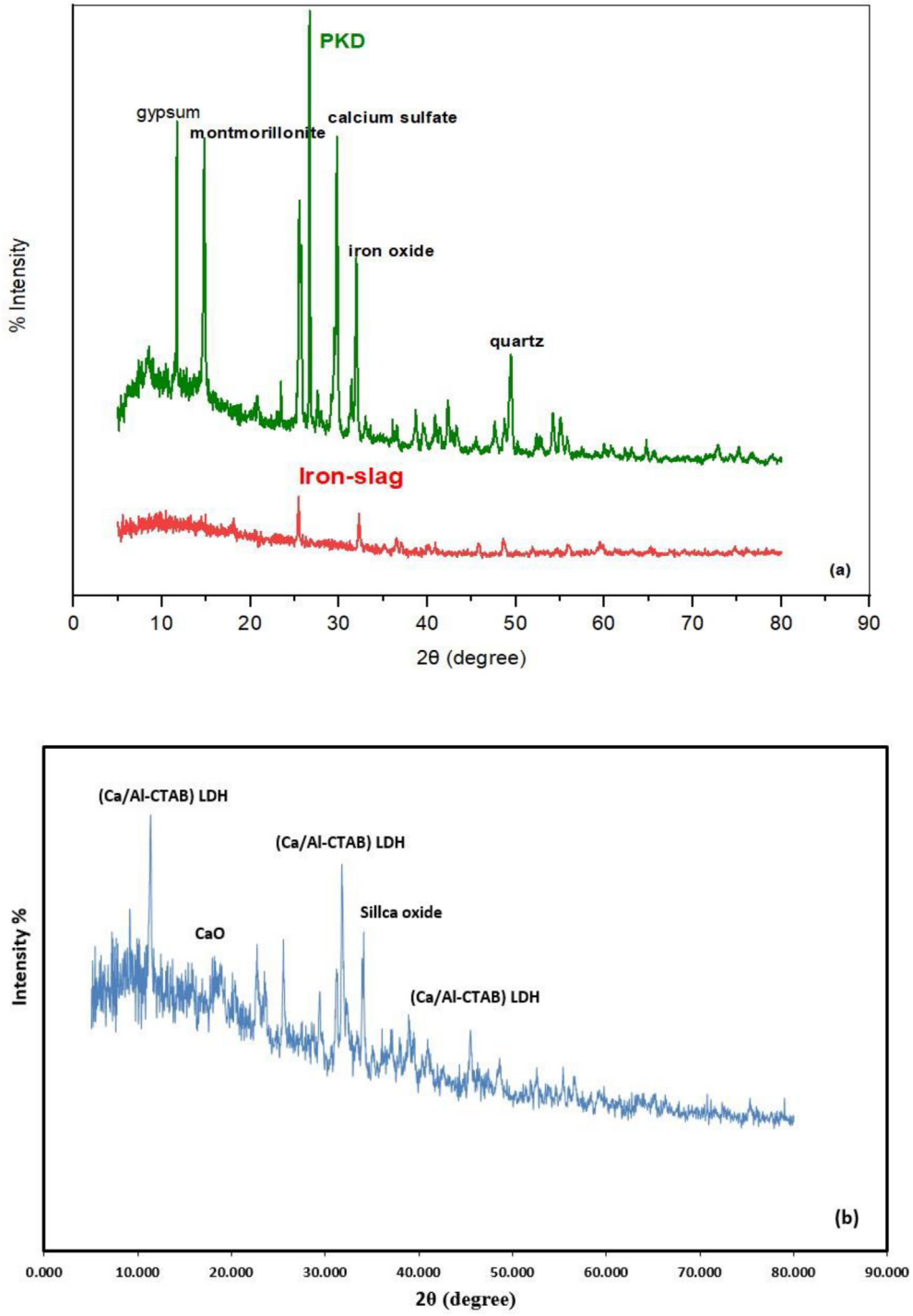

Fig. 3 (a) XRD profile for plaster dust, virgin iron-slag and (b) slag after coating with nanoparticles of layered double hydroxide.

Specific surface area and pore size of the produced sorbent have a considerable effect on its adsorption ability. As a result, these features were assessed by performing BET tests on iron-slag before and after coating. Fig. 4 depicts N_2 adsorption isotherms for PKD, iron-slag, and (Ca/Al - CTAB- LDH) coated with iron-slag samples. Adsorption-desorption isotherm curves of Nitrogen gas to these sorbents correspond for type IV for (p/p_0) values ranging from 0.0 to 1. Microspore volume, total pore volume (p/p_0 = 0.990), and average pore diameter are equal to 0.112, 0.002, and 15.507 for pristine slag; however, these characteristics have increased for coated slag to be 2.346 cm^3/g, 0.057 cm^3/g, and 22.525 nm respectively.

FESEM plots are described the morphology of PKD as shown in Fig. 5a with BET (7.336 m^2/g), virgin iron-slag Fig. 5b, (Ca/Al - CTAB- LDH) coated with iron-slag Fig. 5c, and enhanced adsorption of Cd contaminated on coated iron-slag Fig. 5d. The porous surface of iron-slag has a nonhomogeneous morphology; yet, the surface structure

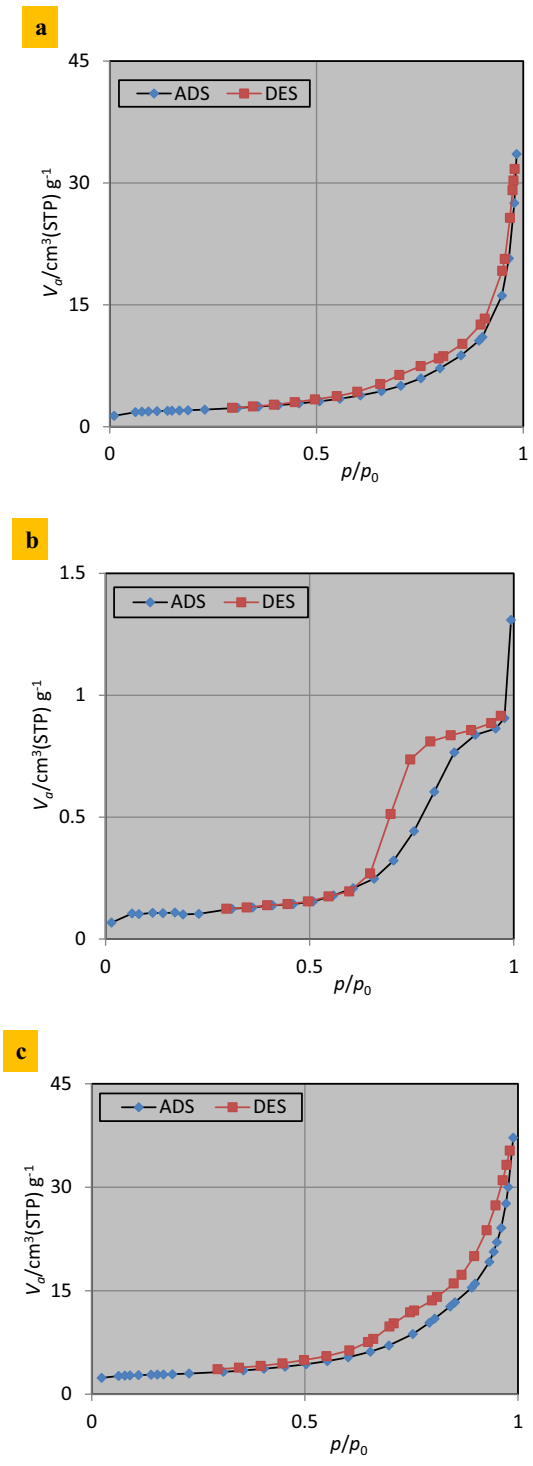

Fig. 4 N_2 adsorption–desorption isotherms for (a) PKD, (b) virgin iron-slag, (c) (Ca/Al - CTAB- LDH) coated with iron-slag.

seems to be very compact and chaotic. Surface roughness and iron-slag fissures were clearly visible. Fig. 5b depicts the creation of layers with asymmetric orientations and sizes (Amaniampong et al., 2018). Adsorbent efficiency can be improved by increasing the surface area that is subject to interaction with contaminant. In comparison with sorbent before interaction with contaminant, sorbent morphology was clearly changed Fig. 5d as a result to binding of contaminant molecules with sorbent after sorption process. This observation is in-line with change in surface area determined from BET test as explained previously.

EDX yields elemental composition graphs for PKD, virgin iron-slag, and composite sorbent before and after to sorption process, as clear from Fig. 6. The primary components in representative iron-slag grains are Ti, O, Si, Fe, k, Al, C, Ca, Mg, Na, and Mn. Iron content was (7%), this is consistent with previous studies (Faisal et al., 2022a, 2022b, 2022c). Tables in Fig. 6 show that the percentages of Ca in coated iron-slag increased considerably from 3.5 to 18.0%, whereas the percentages of Al were 17.7%. This increase demonstrates the success of the plantation's layered double hydroxides. As seen in Fig. 6d, a cloud of cadmium form on iron-slag particles loaded with cadmium with about 7.4%.

4.2. Sorbent manufacturing

To synthesize of coated slag, the influences of CTAB mass, pH, Ca/Al molar ratio, and iron-slag dosage on the prepared sorbent were tested. The highest sorption efficiency of cadmium was the indictor adopted to determine the suitable values of these conditions. Three CTAB masses (0, 0.035, and 0.05 g) were used with Ca/Al molar ratio 2, iron-slag dosage of 1 g/50 mL, pH = 10, C_o = 50 mg/L, and time 3 h at 250 rpm. Fig. 7a depicts changes in cadmium removal versus CTAB mass. However, without the addition of CTAB surfactant, modification of iron-slag surfaces by precipitation of (Ca/Al)-LDH nanoparticles can boost the removals 80% Cd. The CTAB at 0.035 g may boost cadmium removals to the greatest value of 98.3%. This increase could be attributed to the increase of spacing for the Ca/Al layer in the existence of CTAB, that improves the adsorptive properties of the synthesized sorbent (Mierczynska-Vasilev and Smith, 2016). This figure also shows that increasing the CTAB dose over 0.035 g may result in a significant reduction in pollutants removal because of the formation of electrostatic disharmony forces among cations existing within sorbent and contaminant.

To find influence of solution pH on efficacy of prepared sorbent, preparation tests are conducted with three values of pH specifically 9, 10, and 11, at (Ca/Al) molar ratio 2 and slag dosage 1 g/ 50 mL, C_o = 50 mg/L, and t = 3 h for 250 rpm. Fig. 7b depicts the relationship between cadmium removals and the pH utilized in the synthesis method. The maximum capabilities were identified at an initial pH of 10 with values equal to 98.3% for Cd. Increase or decrease in pH from 10 could result in a significant drop in this ability as no all nanoparticle would be bonded to the iron-slag surface or enhancing nanoparticle diameter; thus, the optimal coating process could be obtained at pH 10.

Three (Ca/Al) molar ratios, 1, 2, and 3, were used for pH at 10 and slag dosage of 1 g/50 mL. Fig. 7c shows that highest removals (98.3% cadmium) happened at (Ca/Al-CTAB) molar ratio equal to 2 because of the high interactions between pollutant and surface area for sorption tests at the same conditions indicated in stages. An increment or reduction in molar ratio from 2 is linked to a drop in pollutant removal. The instability of LDH's layered hydrotalcite-like composition or variations in radius difference between Calcium and Aluminum could be main causes of this drop (Xu and Zeng, 2001).

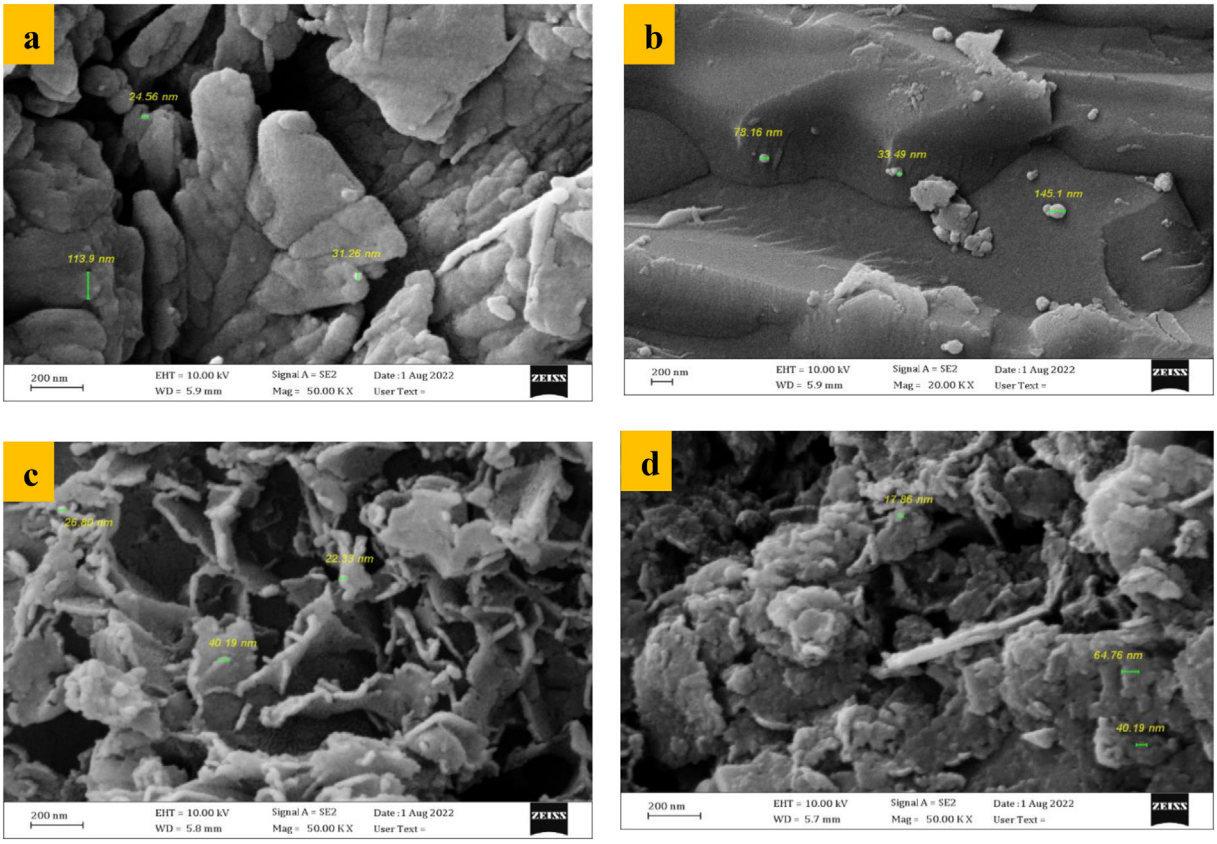

Fig. 5 FESEM images for (a) PKD, (b) virgin iron-slag, (c) (Ca/Al - CTAB- LDH) coated with iron-slag, (d) coated iron-slag loaded with Cd^{+2}.

Impact of iron-slag dosage (adjusted from 0.5 to 1.5 g/50 mL) on sorbent manufacture using the same preparation circumstances steps CTAB dosage should be set at 0.035 g, pH at 10, and Ca/Al molar ratio at 2. Fig. 7d depicts the amounts of removal percentage owing to changes in sludge doses for sorption experiments performed. It appears that 1 g of iron-slag each 50 mL of solution used to produce iron slag - (Ca/Al-CTAB)-LDH can extract the largest amount of cadmium with efficiency of 98.3%. A decrement in iron-slag quantity from g is linked to a significant decrease in removal percent's, which may be attributed to the fact that several (Ca/Al-CTAB) nanoparticles aren't given the possibility to attach to the surfaces of iron-slag and will thus be removed during the washing process. This figure also shows that removal of pollutants has been reduced for iron-slag dosages greater than 1 g due to an increase in surface area for the identical amount of Nano-particles as compared to the best one.

4.3. Operation parameters in batch testing program

To guarantee that equilibrium concentration are achieved in batch experiments, contact time must have kept at an acceptable value. Fig. 8a depicts the variation in the relation between percentage removal and contact time when 0.5 g of iron-slag-(Ca/Al-CTAB)-LDH was mixed with 50 mL of polluted solution at room temperature, C_o 50 mg/L, initial pH 7, and agitation speed of 250 rpm. This figure clearly shows that the adsorption rate was really quite quick at first and increased as the contact time till it reached equilibrium, indicating a gradual blinding of sorption sites on the adsorbent surface. Within one hour, 99.3% of the cadmium was eliminated. While residual concentrations of these chemical species were kept mostly constant after 2 h of contact time with minor fluctuations up to 3 h. The existence of a sufficient number of reactive binding sites on the sorbent surface may explain the high rate of adsorption. As a result, the contact time of one hour can be used for subsequent sorption experiments because it was found to be sufficient to reach equilibrium.

The role of sorbent mass in the elimination of cadmium in the range (0.01–1 g) added to 50 mL at 250 rpm for C_o 50 mg/L was investigated following the specifying of the optimal contact time values. The findings (Fig. 8b) indicated that the 0.01 g of prepared sorbent can merely remove 44% target metal; However, the sorption efficiency of this metal can be significantly improved to 99.3 percent by increasing sorbent mass to 0.5 g. This is logic behavior because the increasing of sorbent mass means the increase of the vacant sites for capturing of contaminant (Amarasinghe and Williams, 2007). Because the cadmium concentrations distributed between the sorbent and the aqueous solution remain constant even with further mass addition, the results demonstrated that an increase in the quantity of sorbent above 0.5 g will not have any effect on the Cd removal percentages (Unuabonah et al., 2008).

The pH value impacts the surface structure of sorbents, the production of metal hydroxides, and the interaction between

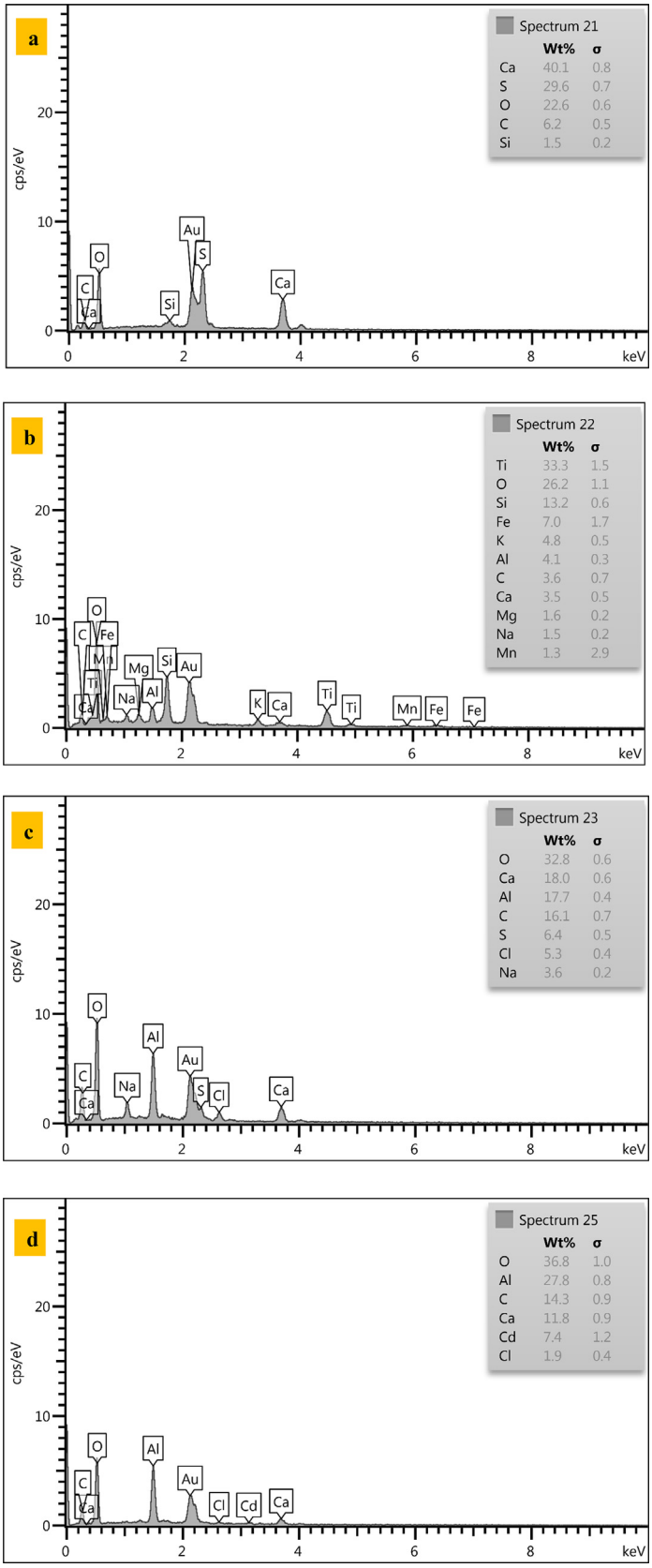

Fig. 6 EDX images for (a) PKD, (b) virgin iron-slag, (c) (Ca/Al-CTAB) LDH coated with iron-slag, (d) coated iron-slag loaded with Cd.

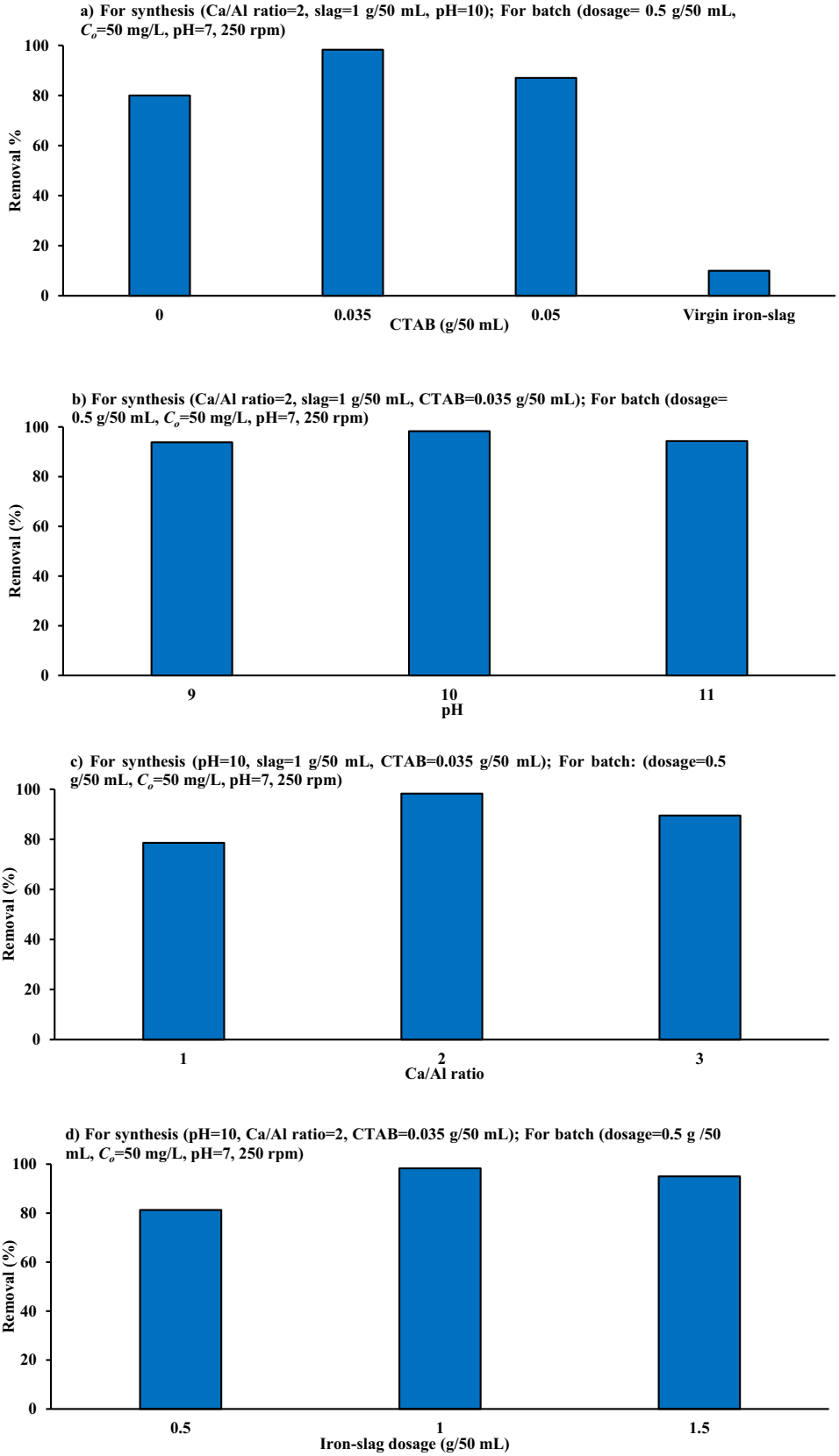

Fig. 7 Influences of a) CTAB b) pH, c) Ca/Al ration and d) iron-slag mass on the Cd^{+2} removal efficiency by coated slag.

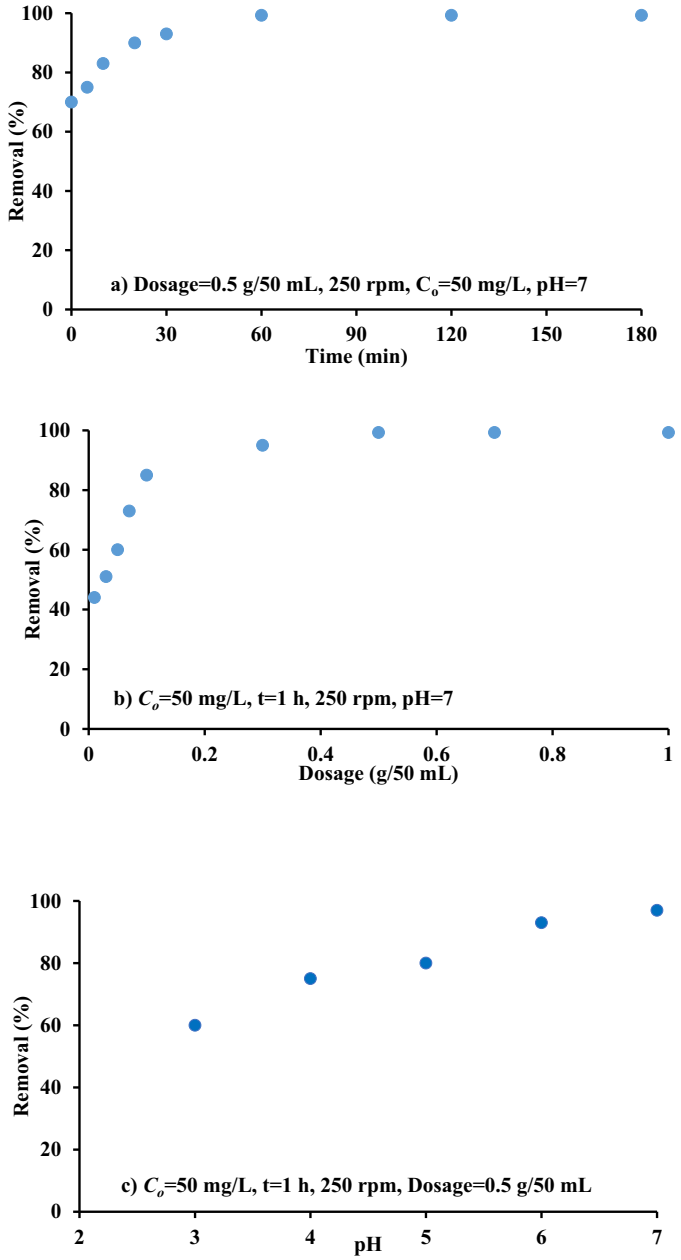

Fig. 8 Effect of a) contact time, b) iron-slag-(Ca/Al-CTAB)-LDH dosage, c) pH d) initial concentration e) agitation speed on the cadmium ions removal from aqueous solution.

sorbents and metal ions. This is because the protonation and deprotonation of the acidic and basic groups of the adsorbents changes their sorption behavior for metal ions. Consequently, the pH reliance of sorption for metal particles was researched. The sorption of cadmium on iron-slag-(Ca/Al-CTAB)-LDH in the initial pH range 3–7 for a dose of 0.5 g/50 mL at a constant initial ionic concentration of 50 mg/L and shaking speed of 250 rpm (Fig. 8c). This figure shows that the sorption behavior of metal ions is more sensitive to pH changes.

It is necessary to modify the natural materials with nanoparticles to obtain higher adsorption capacity. The CTAB as cationic surfactant was added to increase anionic retention, hydrophobicity and cation exchange capacity, and following that increase the electrostatic forces between sorbent and Cd^{+2}. The next tests were implemented at pH 7 to avoid the cadmium precipitation. It is clear that the rising pH values inside the trial scope of (3–7) maintain the increasing of cadmium removal due to a reduce in the liberation of hydrogen ions in the aqueous solution. Up to a pH of 7, cadmium sorption has been observed to generally increase with increasing solution pH. The solution does not contain any hydroxo complexes with a pH below 7; There are only dissociated Cd(II) ions that form aqua ions. Thus, the higher removal of the metal as the pH increments can be made sense of based on a reduction in competitive among proton and metal species for the surface sites, and by reducing in positive surface charge. It is anticipated that the removal efficiency would decrease as pH values rise further. This could be because negative cad-

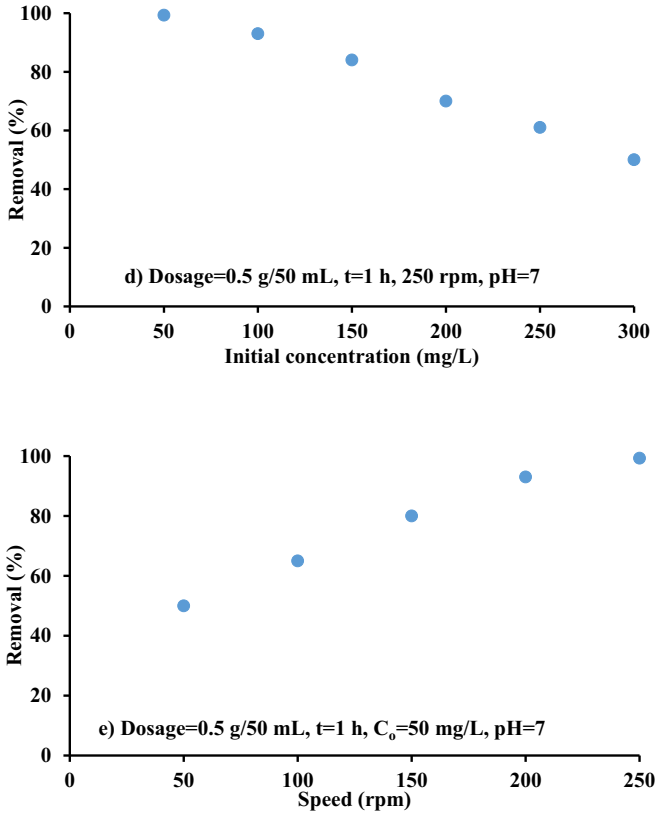

Fig. 8 (*continued*)

mium hydroxides, such as $Cd(OH)_2$, are formed and precipitated from the solution, rendering true sorption studies impossible. Additionally, a surplus of protons can effectively compete with the Cd(II) ions for binding sites on the iron-slag surface at low pH values. The reduction in removal efficiency has been attributed to the surface binding of low-affinity surface sites as high-affinity ones begin to reach saturation. These cation adsorption reactions contribute in releasing hydrogen ions on the surface causing the formation of two types of complex combinations: An outer sphere complex in which the cation binds with anionic sorbent without displacing a water molecule. While in the case of inner sphere complex, the cation binds closely to the anionic adsorbent and displace a water molecule. At a higher concentration of cadmium ions, some molecules of cadmium hydroxide remain insoluble. In the cadmium solution/hydroxyapatite system, cationic exchange process occurs between cadmium and calcium due to the sparingly soluble nature of the hydroxyapatite. The adsorption of cadmium onto sorbent surface of the hydroxyapatite undergoes through various adsorption processes including surface complexation, ion exchange, co-precipitation, and recrystallization (Smičiklas et al., 2000).

The effect of initial cadmium concentration on sorption efficiency of these contaminants onto iron-slag-(Ca/Al-CTAB)-LDH is shown in Fig. 8d. These experiments were conducted using C_o ranging from 50 to 300 mg/L and shaken for 1 h at 250 rpm. The cadmium removal decreased from 99.3% to 50% with the increase of C_o. This means that the amount of metal ions sorbed per unit mass of sorbent decreased with the increase in initial concentration. This indicates that less favorable sites became involved in the process as concentration increased, indicating that the iron-slag samples' active sites for interaction with contaminant have reached saturation (Qadeer and Rehan, 2002).

The effect of agitation speed on the Cd removal efficiency was studied in the range (50–250) rpm and maintaining remaining conditions equal to best ones specified from mentioned steps. Fig. 8d shows that the Cd uptake increases with the increase in shaking rate. There was gradual increase in metal ions uptake with increase of agitation speed until reaching 250 rpm. The speed can improve the metal diffusion towards the coated slag surface. Thus, suitable contact can generate between Cd ions and sites on the sorbent, which can facilitate the transfer of ions to the sorbent. Therefore, higher Cd uptake could be occurred at this speed as it will assure that all sites are readily available for uptake of metal ions.

4.4. Sorption isotherms

The transport equation's reaction term must be described using isotherms in order to determine how the reaction will affect the spread of contaminants in a packed bed. The sorption measurements for Cd^{+2} onto coated slag are fitted with Freundlich and Langmuir models in nonlinear forms using "Solver" option. The results of fitting process listed in Table 1 are represented the constants of isotherm models. The table proves that the Langmuir expression is more representative

Table 1 Values of constants for equilibrium sorption models after fitting with measurements of Cd^{+2} ions sorption onto coated iron-slag.

Model	Parameter	Value
Freundlich	K_f (mg/g)(L/mg)$^{1/n}$	2.51
	n	2.49
	R^2	0.97
Langmuir	q_m (mg/g)	14.50
	b (L/mg)	0.48
	R^2	0.99

Table 2 Sorption capacity for cadmium ions onto coated slag in comparison with capacities of other sorbents from previous literatures.

Sorbent	q_m (mg/g)	Reference
Moroccan stevensite	22.37	(Benhammou et al., 2005)
Impregnated styrofoam	29.11	(Memon et al., 2006)
Biopolymer-coated hydroxyapatite foams	35.52	(Vila et al., 2011)
Flour-hydroxyapatite composites	193.84	(Zhu et al., 2017)
Mg–Fe-LDH-RHA	28.90	(Yu et al., 2018)
KB/LDH	25.60	(Tan et al., 2019)
Filter cake coated by hydroxyapatite	34.72	(Ahmed et al., 2020)
Iron-slag coated with (Ca/Al-CTAB) LDH	14.50	Present study

for sorption outputs in comparison with Freundlich model specially $R^2 = 0.99$; however, the concurrence between model curve and measurements can illustrate in Fig. 9. Isotherm models are very important for description of reaction term in the solute transport equation through the packed beds like migration of contaminant in the subsurface environment.

Based on the separation factor ($Sf = 1/(1 + bC_o)$) calculated with aid of Langmuir model, the curves of sorption are identified as "favorable" because the values of Sf ranged from 0 to 1 (Rai et al., 2016). Table 2 confirm that the measured maximum adsorption capacities are consistent with values listed in previous literatures for various materials. Thus, the coated iron-slag prepared from industrial products can use as alternative for several industrial sorbents. The Freundlich parameter (K_f) was equal to 2.51 (mg/g) (L/mg)$^{1/n}$ onto prepared sorbent while the value of constant (n) > 1 which means "favorable" adsorption of contaminant onto the coated iron-slag.

4.5. Sorption kinetics

Sorption kinetics provides rate of cadmium uptake onto sorbent particles and, consequently, affects equilibrium time. Kinetic modelling of sorption process can be used to determine uptake mechanism that governs transport of contaminants from aqueous solution to sorbent material. In this modeling, sorption process is dependent on reactions occurring on surface of sorbent. Most frequently considered kinetic models for sorption include pseudo-first-order and pseudo-second-order kinetic expressions. Prediction of rate sorption of dissolved pollutants from liquid phase is very important in design of appropriate treatment processes (Qiu et al., 2009).

Fig. 10 illustrates kinetic models that fit experimental data of cadmium sorption onto surface of (Ca/Al-CTAB) LDH nanoparticles. Table 3 shows constants for these models as obtained via a fitting process in Excel 2016 using the nonlinear regression-solver option. For the largest value of R^2, and closest match of q_e to test data, the pseudo second-order model is shown to be the most acceptable strategy for de scribing kinetics involved in sorption process to investigated pollutants. This means that chemisorption is primary mechanism, with valence force acting as a rate-determining step in sorption process by spreading or exchanging electrons between active sites of sorbent and sorbate (Komy et al., 2014). Models of kinetics alone would be insufficient for describing mechanisms involved in

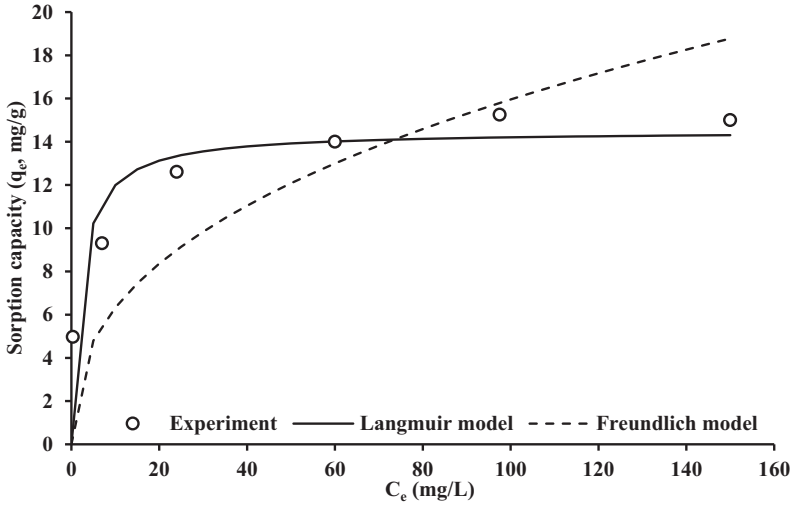

Fig. 9 Sorption isotherms for cadmium – coated slag interaction in comparison with measurements.

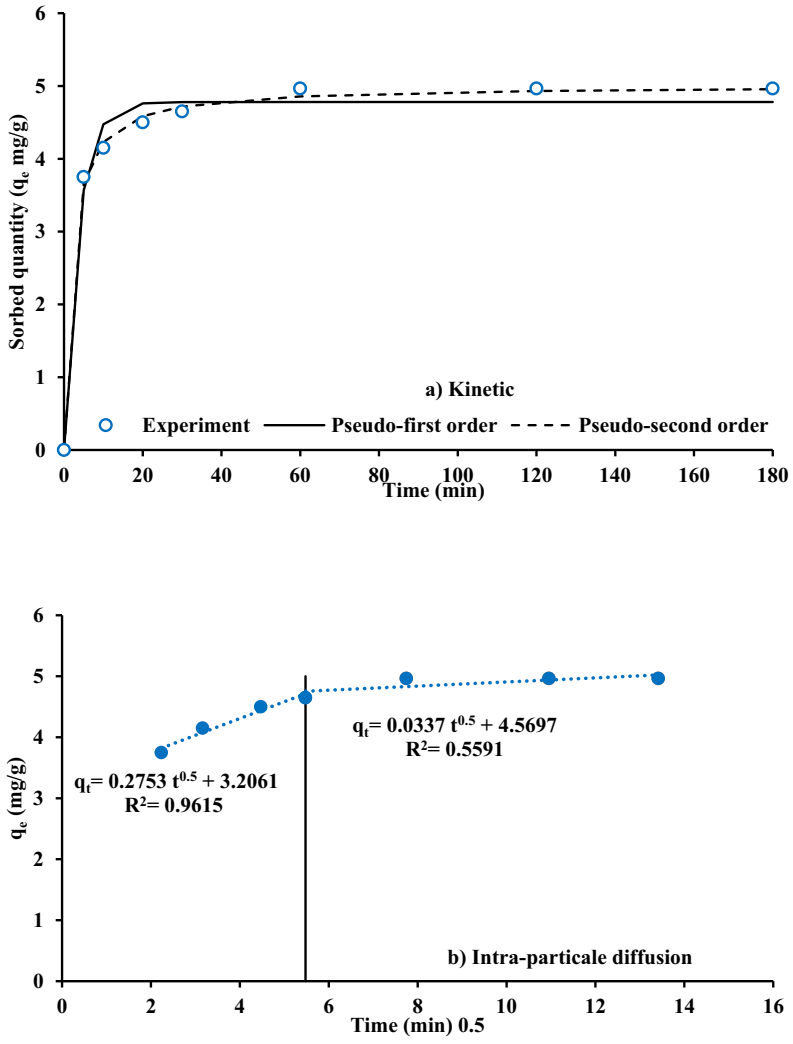

Fig. 10 Formulation of kinetic measurements for sorption of Cd^{+2} ions onto the coated iron-slag.

Table 3 Values of constants for kinetic sorption models after fitting with measurements of Cd^{+2} ions sorption onto coated iron-slag.

Model	Parameter	Value
Pseudo-first-order	q_e	4.78
	k_1	0.28
	R^2	0.98
	SSE	12.57
Pseudo-second-order	q_e	5.01
	K_2	0.11
	R^2	0.99
	SSE	12.29
Intra-particle diffusion	Portion 1	
	k_{int} (mg/g $min^{0.5}$)	0.2753
	C	3.2061
	R^2	0.9615
	Portion 2	
	k_{int} (mg/g $min^{0.5}$)	0.0337
	C	4.5697
	R^2	0.5591

sorption processes, necessitating the use of the diffusion of intra-particles model developed by (Weber and Morris, 1962). This model's empirical formula connects adsorbed amount with $t^{0.5}$ value rather than t, as follows:

$$q_t = k_{int} t^{0.5} + C \quad (7)$$

where k_{int} symbolizes rate constant for sorption in this model (mg/g $min^{0.5}$), and C is intercept value refers to thickness of boundary layer.

Intra-particle diffusion model, straight line relationship between q_t values versus $t^{0.5}$, for tested metal is plotted in Fig. 10. The straight-line plots do not pass through origin, clearly suggesting that intra-particle diffusion is involved in adsorption process but rate-controlling step will not be represented. Furthermore, plots in this figure show multi-linearity, indicating a regulated process of cadmium adsorption via two or more simultaneous processes. Accordingly, adsorption mainly occurs by surface complexation and ion exchange, and follows both pseudo second-order and intra-particle diffusion kinetic models (Cheung et al., 2007; Elkady et al., 2011).

4.6. Recyclability

To evaluate the possibility of reuse exhausted iron-slag coated with (Ca/Al-CTAB)-LDH for removal Cd, set of experimental tests were conducted. These tests depend on implementation of the adsorption and de-sorption cycles. The regeneration process is based on desorb of contaminant from exhausted sorbent by utilizing 0.5 M HCl. Fig. 11 shows that the removal percentages of Cd as function for number of recycle times which reflect regeneration efficiency of iron-slag coated with (Ca/Al-CTAB)-LDH. It is obvious that efficiencies were reduced with numbers of recycles and more than 90% can remove until 6 cycles. Findings indicated that prepared sorbent had a suitable reusability; and has high reliability and can be applied effectively in the restoration of water contained Cd contaminates especially in field practical.

4.7. Treatment of groundwater

To make this study more accurate and reliable, water samples were taken from a well in the Babylon Governorate-Iraq at the coordinates 33.439, 44.623 in order to evaluate iron-slag coated with (Ca/Al-CTAB) LDH ability to clean up real groundwater that had been contaminated with cadmium. The characteristics of this water have measured which included pH, electrical conductivity (EC), Turbidity, total dissolved solid (TDS), total suspended solids (TSS), hardness, sulfate (SO_4^{-2}), calcium (Ca^{+2}), magnesium (Mg^{+2}), and Chloride (Cl^{-1}). The values of these characteristics are 7.3, 2.37 mS/cm, 21.98 NTU, 2120 mg/L, 953.4 mg/L,760 mg/L, 692 mg/L, 280.6 mg/L, 13.5 mg/L, and 525 mg/L respectively. The conditions of these experiments are the same ones achieved the highest removal percent that obtained from batch tests (initial concentration 50 mg/L, mass 0.5 g/50 mL, 250 rpm, t = 1 h, pH 7). The removal percentage of cadmium ions onto coated slag was dropped to 81.5% for real groundwater in comparison with 99.3% for DW. This finding is logical because of the competition between the chemicals presented in the actual groundwater which can cause the mentioned reduction in the removal percentage.

5. Conclusions and future directions

In the presence of CTAB surfactant, the successful green production of (Ca/Al) nanoparticles by combining the aluminum produced by the dissolution of alum with calcium extracted from plaster kiln dust byproduct was made possible. The particles are immobilized on the iron-slag solid matrix to obtain innovative sorbent identified as "iron-slag coated with (Ca/Al-CTAB) LDH" to satisfy the objective of this work that can contribute in the applications of sustainable development. The preparation of such sorbent requires the best conditions CTAB mass 0.035 g/50 mL, iron-slag dosage 1 g/50 mL, and (Ca/Al) molar ratio 2 at pH 10 to remove highest value of cadmium ions. Coated sludge and cadmium-containing water interact best under initial pH 7, a sorbent dosage of 0.5 g/50 mL, and a speed of 250 rpm for one hour and C_o 50 mg/L to ensure greater than 99 percent removal efficiency. The outcomes of sorption process were well fitted with Langmuir isotherm to be the highest value of sorption capacity of 14.50 mg/g. Kinetic outputs signified that the model of pseudo-second-order can describe in precise manner the sorption measurements and the removal of cadmium occurred by "chemisorption" process. Examinations of materials before and after coating have demonstrated that the covering of slag was accurately accomplished because of increment the Ca^{+2} and Al^{+3} rates as well as the alteration of iron-slag can connect with critical expansion in the surface region from 0.49 to 10.21 m^2/g. According to the FT-IR spectrum, electrostatic attraction and hydrogen bonding are controlling the sorption of Cd^{+2} onto prepared sorbent. Also, the exhausted slag can reuse and its efficiency was greater than 83% after 9 cycles of regeneration. The main recommendation for future studies is used the coated slag in the in situ permeable reactive barrier technology to treat the real groundwater in the field operation mode.

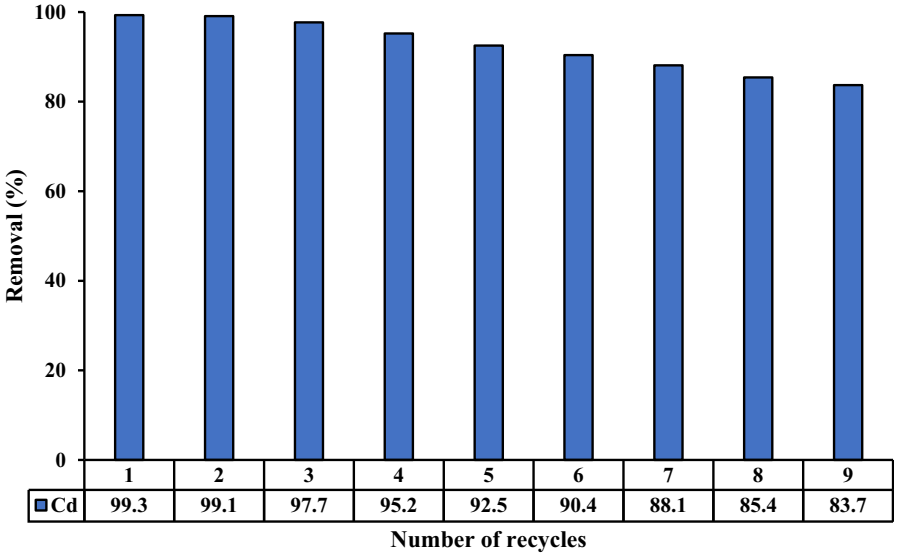

Fig. 11 Removals of Cd from contaminated groundwater onto iron-slag coated with (Ca/Al-CTAB) LDH versus the regeneration cycle.

Declaration of Competing Interest

The authors declare that they have no known competing financial interests or personal relationships that could have appeared to influence the work reported in this paper.

References

Ahmed, D.N., Faisal, A.A.H., Jassam, S.H., Naji, L.A., Naushad, M., 2020. Kinetic model for pH variation resulted from interaction of aqueous solution contaminated with nickel ions and cement kiln dust. J. Chem. 2020, 1–11. https://doi.org/10.1155/2020/8732308.

Amaniampong, P.N., Trinh, Q.T., Varghese, J.J., Behling, R., Valange, S., Mushrif, S.H., Jérôme, F., 2018. Unraveling the mechanism of the oxidation of glycerol to dicarboxylic acids over a sonochemically synthesized copper oxide catalyst. Green Chem. https://doi.org/10.1039/c8gc00961a.

Amarasinghe, B., Williams, R.A., 2007. Tea waste as a low cost adsorbent for the removal of Cu and Pb from wastewater. Chem. Eng. J. 132, 299–309.

Basibuyuk, M., Kalat, D.G., 2004. The use of waterworks sludge for the treatment of vegetable oil refinery industry wastewater. Environ. Technol. 25, 373–380. https://doi.org/10.1080/09593330409355471.

Behbahani, M., Rabiee, G., Bagheri, S., Amini, M.M., 2022. Ultrasonic-assisted d-μ-SPE based on amine-functionalized KCC-1 for trace detection of lead and cadmium ion by GFAAS. Microchem. J. 183, 107951. https://doi.org/10.1016/j.microc.2022.107951.

Benhammou, A., Yaacoubi, A., Nibou, L., Tanouti, B., 2005. Adsorption of metal ions onto Moroccan stevensite: kinetic and isotherm studies. J. Colloid Interface Sci. 282, 320–326. https://doi.org/10.1016/j.jcis.2004.08.168.

Cheung, W.H., Szeto, Y.S., McKay, G., 2007. Intraparticle diffusion processes during acid dye adsorption onto chitosan. Bioresour. Technol. 98, 2897–2904. https://doi.org/10.1016/j.biortech.2006.09.045.

Colangelo, F., Cioffi, R., 2013. Use of cement kiln dust, blast furnace slag and marble sludge in the manufacture of sustainable artificial aggregates by means of cold bonding pelletization. Materials (Basel). 6, 3139–3159.

Dinari, M., Neamati, S., 2020. Surface modified layered double hydroxide/polyaniline nanocomposites: Synthesis, characterization and Pb2+ removal. Colloids Surf. A Physicochem. Eng. Asp. 589, 124438. https://doi.org/10.1016/j.colsurfa.2020.124438.

Elkady, M.F., Mahmoud, M.M., Abd-El-Rahman, H.M., 2011. Kinetic approach for cadmium sorption using microwave synthesized nano-hydroxyapatite. J. Non. Cryst. Solids 357, 1118–1129. https://doi.org/10.1016/j.jnoncrysol.2010.10.021.

Faisal, A., Ahmed, M., 2014. Remediation of groundwater contaminated with copper ions by waste foundry sand permeable barrier. J. Eng. 20, 62–77.

Faisal, A.A.H., Hmood, Z.A., 2015. Groundwater protection from cadmium contamination by zeolite permeable reactive barrier. Desalin. Water Treat. 53. https://doi.org/10.1080/19443994.2013.855668.

Faisal, A.A.H., Naji, L.A., 2019. Simulation of ammonia nitrogen removal from simulated wastewater by sorption onto waste foundry sand using artificial neural network. Assoc. Arab Univ. J. Eng. Sci. 26, 28–34. https://doi.org/10.33261/jaaru.2019.26.1.004.

Faisal, A.A.H., Nassir, Z.S., 2016. Modeling the removal of cadmium ions from aqueous solutions onto olive pips using neural network technique. Al-Khwarizmi Eng. J. 12, 1–9.

Faisal, A.A.H., Nassir, Z.S., Naji, L.A., Naushad, M., Ahamad, T., 2020. A sustainable approach to utilize olive pips for the sorption of lead ions: numerical modeling with aid of artificial neural network. Sustain. Chem. Pharm. 15. https://doi.org/10.1016/j.scp.2020.100220.

Faisal, A.A.H., Ahmed, D.N., Saleh, B., Afzal, A., Sharma, G., 2022a. Elimination of hazard cadmium ions from simulated groundwater using hydroxyapatite coated filter cake made of sewage sludge and cement kiln dust. J. Polym. Environ. 30, 1478–1490. https://doi.org/10.1007/s10924-021-02286-0.

Faisal, A.A.H., Nassir, Z.S., Rashid, H.M., Al-Hashimi, O.A., Shubbar, A., Saleh, B., 2022b. Neural network for modeling the capture of lead and cadmium ions from wastewater using date palm stones. Int. J. Environ. Sci. Technol. 19, 10563–10576. https://doi.org/10.1007/s13762-021-03883-1.

Faisal, A.A.H., Ramadhan, Z.K., Al-Ansari, N., Sharma, G., Naushad, M., Bathula, C., 2022c. Precipitation of (Mg/Fe-CTAB) - Layered double hydroxide nanoparticles onto sewage sludge for producing novel sorbent to remove Congo red and methylene blue dyes from aqueous environment. Chemosphere 291, 132693. https://doi.org/10.1016/j.chemosphere.2021.132693.

Ghodsi, S., Behbahani, M., Yegane Badi, M., Ghambarian, M., Sobhi, H.R., Esrafili, A., 2021. A new dendrimer-functionalized magnetic nanosorbent for the efficient adsorption and subsequent trace measurement of Hg (II) ions in wastewater samples. J. Mol. Liq. 323, 114472. https://doi.org/10.1016/j.molliq.2020.114472.

Ghorbani-Kalhor, E., Behbahani, M., Abolhasani, J., Hosseinzadeh Khanmiri, R., 2015. Synthesis and characterization of modified multiwall carbon nanotubes with Poly (N-Phenylethanolamine) and their application for removal and trace detection of lead ions in food and environmental samples. Food Anal. Methods 8, 1326–1334. https://doi.org/10.1007/s12161-014-0001-x.

Guo, Y., Zhu, Z., Qiu, Y., Zhao, J., 2012. Adsorption of arsenate on Cu/Mg/Fe/La layered double hydroxide from aqueous solutions. J. Hazard. Mater. 239–240, 279–288. https://doi.org/10.1016/j.jhazmat.2012.08.075.

He, X., Qiu, X., Chen, J., 2017. Preparation of Fe(II)–Al layered double hydroxides: application to the adsorption/reduction of chromium. Colloids Surfaces A Physicochem. Eng. Asp. 516, 362–374. https://doi.org/10.1016/j.colsurfa.2016.12.053.

He, X., Qiu, X., Hu, C., Liu, Y., 2018. Treatment of heavy metal ions in wastewater using layered double hydroxides: a review. J. Dispers. Sci Technol. https://doi.org/10.1080/01932691.2017.1392318.

Hilal, N.M., Ahmed, I.A., El-Sayed, R.E., 2012. Activated and nonactivated date pits adsorbents for the removal of copper(II) and cadmium(II) from aqueous solutions. Int. Sch. Res. Not. 2012, 1–11. https://doi.org/10.5402/2012/985853.

Kheradmand, A., Negarestani, M., Kazemi, S., Shayesteh, H., Javanshir, S., Ghiasinejad, H., Jamshidi, E., 2023. Design and preparation magnetic bio-surfactant rhamnolipid-layered double hydroxide nanocomposite as an efficient and recyclable adsorbent for the removal of Rifampin from aqueous solution. Sep. Purif. Technol. 304, 122362. https://doi.org/10.1016/j.seppur.2022.122362.

Khitous, M., Salem, Z., Halliche, D., 2016. Removal of phosphate from industrial wastewater using uncalcined MgAl-NO 3 layered double hydroxide: batch study and modeling. Desalin. Water Treat. 57, 15920–15931. https://doi.org/10.1080/19443994.2015.1077745.

Koldabadi, S.G., Ruchi, V., Bhaskar, K.V., Lalit, K., 2012. Heavy metals in environment, living systems and herbal preparation: an overview. Int. Res. J. Pharm. 3, 128–130.

Komy, Z.R., Shaker, A.M., Heggy, S.E.M., El-Sayed, M.E.A., 2014. Kinetic study for copper adsorption onto soil minerals in the absence and presence of humic acid. Chemosphere 99, 117–124. https://doi.org/10.1016/j.chemosphere.2013.10.048.

Le-ping, L., Xue-min, C., Shu-heng, Q., Jun-li, Y., Lin, Z., 2010. Preparation of phosphoric acid-based porous geopolymers. Appl. Clay Sci. 50, 600–603. https://doi.org/10.1016/j.clay.2010.10.004.

Liang, X., Zang, Y., Xu, Y., Tan, X., Hou, W., Wang, L., Sun, Y., 2013. Sorption of metal cations on layered double hydroxides. Colloids Surf. A Physicochem. Eng. Asp. https://doi.org/10.1016/j.colsurfa.2013.05.006.

Memon, S.Q., Bhanger, M.I., Hasany, S.M., Khuhawar, M.Y., 2006. Sorption behavior of impregnated Styrofoam for the removal of Cd (II) ions. Colloids Surf. A Physicochem. Eng. Asp. 279, 142–148. https://doi.org/10.1016/j.colsurfa.2005.12.052.

Mierczynska-Vasilev, A., Smith, P.A., 2016. Surface modification influencing adsorption of red wine constituents: The role of functional groups. Appl. Surf. Sci. https://doi.org/10.1016/j.apsusc.2016.06.016.

Nava-Andrade, K., Carbajal-Arízaga, G.G., Obregón, S., Rodríguez-González, V., 2021. Layered double hydroxides and related hybrid materials for removal of pharmaceutical pollutants from water. J. Environ. Manage. 288, 112399. https://doi.org/10.1016/j.jenvman.2021.112399.

Normah, N., Juleanti, N., Siregar, P.M.S.B.N., Wijaya, A., Palapa, N. R., Taher, T., Lesbani, A., 2021. Size selectivity of anionic and cationic dyes using LDH modified adsorbent with low-cost rambutan peel to hydrochar. Bull. Chem. React. Eng. Catal. 16, 869–880. https://doi.org/10.9767/bcrec.16.4.12093.869-880.

Proctor, D.M., Fehling, K.A., Shay, E.C., Wittenborn, J.L., Green, J. J., Avent, C., Bigham, R.D., Connolly, M., Lee, B., Shepker, T.O., Zak, M.A., 2000. Physical and chemical characteristics of blast furnace, basic oxygen furnace, and electric arc furnace steel industry slags. Environ. Sci. Technol. 34, 1576–1582. https://doi.org/10.1021/es9906002.

Qadeer, R., Rehan, A.H., 2002. A study of the adsorption of phenol by activated carbon from aqueous solutions. Turk. J. Chem. 26, 357–362.

Qiu, H., Lv, L., Pan, B., Zhang, Q.-J., Zhang, W., Zhang, Q.-X., 2009. Critical review in adsorption kinetic models. J. Zhejiang Univ. A 10, 716–724. https://doi.org/10.1631/jzus.A0820524.

Rai, M.K., Shahi, G., Meena, V., Meena, R., Chakraborty, S., Singh, R.S., Rai, B.N., 2016. Removal of hexavalent chromium Cr (VI) using activated carbon prepared from mango kernel activated with H_3PO_4. Resour. Technol. 2, S63–S70. https://doi.org/10.1016/j.reffit.2016.11.011.

Samra, S.E., Jeragh, B., El-Nokrashy, A.M., El-Asmy, A.A., 2014. Biosorption of Pb^{2+} from natural water using date pits: a green chemistry approach. Mod. Chem. Appl. 02, 1–8. https://doi.org/10.4172/2329-6798.1000131.

Shah, S.S., Sharma, T., Dar, B.A., Bamezai, R.K., 2021. Adsorptive removal of methyl orange dye from aqueous solution using populous leaves: insights from kinetics, thermodynamics and computational studies. Environ. Chem. Ecotoxicol. 3, 172–181. https://doi.org/10.1016/j.enceco.2021.05.002.

Shayesteh, H., Rahbar-Kelishami, A., Norouzbeigi, R., 2016. Evaluation of natural and cationic surfactant modified pumice for congo red removal in batch mode: Kinetic, equilibrium, and thermodynamic studies. J. Mol. Liq. 221, 1–11. https://doi.org/10.1016/j.molliq.2016.05.053.

Shayesteh, H., Raji, F., Kelishami, A.R., 2021. Influence of the alkyl chain length of surfactant on adsorption process: a case study. Surfaces and Interfaces 22, 100806. https://doi.org/10.1016/j.surfin.2020.100806.

Shihab, A.H., Faisal, A.A.H., 2022. Using novel coated sand as reactive bed in permeable barrier for elimination of methyl orange dye from groundwater. Iraqi J. Agric. Sci. 53, 1067–1077. https://doi.org/10.36103/ijas.v53i5.1620.

Smičiklas, I., Milonjić, S., Pfendt, P., Raičević, S., 2000. The point of zero charge and sorption of cadmium (II) and strontium (II) ions on synthetic hydroxyapatite. Sep. Purif. Technol. 18, 185–194. https://doi.org/10.1016/S1383-5866(99)00066-0.

Tan, Y., Yin, X., Wang, C., Sun, H., Ma, A., Zhang, G., Wang, N., 2019. Sorption of cadmium onto Mg-Fe Layered Double Hydroxide (LDH)-Kiwi branch biochar. Environ. Pollut. Bioavailab. 31, 189–197. https://doi.org/10.1080/26395940.2019.1604165.

Tang, Z., Qiu, Z., Lu, S., Shi, X., 2020. Functionalized layered double hydroxide applied to heavy metal ions absorption: a review. Nanotechnol. Rev. 9, 800–819. https://doi.org/10.1515/ntrev-2020-0065.

Tran, H.N., Lin, C.C., Woo, S.H., Chao, H.P., 2018. Efficient removal of copper and lead by Mg/Al layered double hydroxides intercalated with organic acid anions: adsorption kinetics, isotherms, and thermodynamics. Appl. Clay Sci. 154, 17–27. https://doi.org/10.1016/j.clay.2017.12.033.

Tsakiridis, P.E., Papadimitriou, G.D., Tsivilis, S., Koroneos, C., 2008. Utilization of steel slag for Portland cement clinker production. J. Hazard. Mater. 152, 805–811. https://doi.org/10.1016/j.jhazmat.2007.07.093.

Unuabonah, E.I., Adebowale, K.O., Dawodu, F.A., 2008. Equilibrium, kinetic and sorber design studies on the adsorption of Aniline blue dye by sodium tetraborate-modified Kaolinite clay adsorbent. J. Hazard. Mater. 157, 397–409. https://doi.org/10.1016/j.jhazmat.2008.01.047.

Vila, M., Sánchez-Salcedo, S., Cicuéndez, M., Izquierdo-Barba, I., Vallet-Regí, M., 2011. Novel biopolymer-coated hydroxyapatite foams for removing heavy-metals from polluted water. J. Hazard. Mater. https://doi.org/10.1016/j.jhazmat.2011.04.100.

Wang, L., Wang, A., 2008. Adsorption properties of Congo Red from aqueous solution onto surfactant-modified montmorillonite. J. Hazard. Mater. 160, 173–180. https://doi.org/10.1016/j.jhazmat.2008.02.104.

Weber, W., Morris, J., 1962. Advances in water pollution research: removal of biologically resistant pollutant from waste water by adsorption. In Proceedings of the International Conference on Water Pollution Symposium, pp. 231–266.

Xu, Z.P., Zeng, H.C., 2001. Abrupt structural transformation in hydrotalcite-like compounds $Mg_{1-x}Al_x(OH)_2(NO_3)_x$ nH_2O as a continuous function of nitrate anions. J. Phys. Chem. B. https://doi.org/10.1021/jp0029257.

Yu, J., Zhu, Z., Zhang, H., Qiu, Y., Yin, D., 2018. Mg–Fe layered double hydroxide assembled on biochar derived from rice husk ash: facile synthesis and application in efficient removal of heavy metals. Environ. Sci. Pollut. Res. 25, 24293–24304. https://doi.org/10.1007/s11356-018-2500-6.

Zarezade, V., Aliakbari, A., Eshaghi, M., Amini, M.M., Behbahani, M., Omidi, F., Hesam, G., 2017. Application of a new nanoporous sorbent for extraction and pre-concentration of lead and copper ions. Int. J. Environ. Anal. Chem. 97, 383–397. https://doi.org/10.1080/03067319.2017.1315638.

Zhao, D., Sheng, G., Hu, J., Chen, C., Wang, X., 2011. The adsorption of Pb(II) on Mg_2Al layered double hydroxide. Chem. Eng. J. 171, 167–174. https://doi.org/10.1016/j.cej.2011.03.082.

Zheng, H., Liu, D., Zheng, Y., Liang, S., Liu, Z., 2009. Sorption isotherm and kinetic modeling of aniline on Cr-bentonite. J. Hazard. Mater. 167, 141–147. https://doi.org/10.1016/j.jhazmat.2008.12.093.

Zhu, X., Li, J., Luo, J., Jin, Y., Zheng, D., 2017. Removal of cadmium (II) from aqueous solution by a new adsorbent of fluor-hydroxyapatite composites. J. Taiwan Inst. Chem. Eng. 70, 200–208. https://doi.org/10.1016/j.jtice.2016.10.049.

Zubair, M., Daud, M., McKay, G., Shehzad, F., Al-Harthi, M.A., 2017. Recent progress in layered double hydroxides (LDH)-containing hybrids as adsorbents for water remediation. Appl. Clay Sci. https://doi.org/10.1016/j.clay.2017.04.002.

Zwayen, D.M., Alhussainy, H.Y., 2020. Preparation and characterization of plaster kiln dust-Fe_3O_4 magnetic nanoparticles. J. Eng. 26, 110–122. https://doi.org/10.31026/j.eng.2020.11.07.